

# Photoinduced Charge Transfer in Transition Metal Dichalcogenide Quantum Dots

Arun Singh Patel

*Department of Physics, Dyal Singh College, University of Delhi, Lodhi Road, New Delhi – 110003, India<sup>a)</sup>*

Praveen Mishra

*School of Computational & Integrative Sciences, Jawaharlal Nehru University, New Delhi-110067, India*

Anirban Chakraborti

*School of Computational & Integrative Sciences, Jawaharlal Nehru University, New Delhi-110067, India<sup>b)</sup>*

(Dated: 3 June 2024)

In this paper, a charge transfer mechanism in transition metal dichalcogenide (TMDC) quantum dots (QDs) is studied. A common dye, Rhodamine 6G (R6G), has been used as fluorescent molecule and QDs of molybdenum disulfide ( $\text{MoS}_2$ ) and tungsten disulfide ( $\text{WS}_2$ ) have been used as acceptors of electrons in the photo-induced charge transfer process. The  $\text{MoS}_2$  and  $\text{WS}_2$  QDs have been synthesized using ultrasonication method. These QDs have been characterized using transmission electron microscope (TEM), UV-Vis spectrophotometer, and fluorimeter. The TEM images of these QDs show well dispersed particles of size 2 nm. These QDs show intense fluorescence emission when excited with light having wavelength,  $\lambda < 350$  nm. In presence of light, the photons help in creating charges in fluorescent dye molecule, and TMDCs QDs facilitate the charge transfer in the process. The charge transfer phenomenon has been studied using time correlated single photon counting (TCSPC) set-up, which is a time resolved fluorescence spectroscopic technique. The time resolved fluorescence study shows a drastic change in the fluorescence (FL) lifetime of R6G molecules in the presence of QDs. This decrease in FL lifetime of R6G shows that the  $\text{MoS}_2$ , and  $\text{WS}_2$  QDs provide additional path to the photo-generated electrons in the excited state of R6G. This study can be further extended to optoelectronic devices, where charge transfer plays an important role in the device efficiency and performance.

In recent years, various types of quantum dots (QDs) have been widely explored due to their vast applications in the field of cell imaging, photovoltaic devices, light emitting devices, etc.<sup>1-7</sup> The most attractive property of these materials are being size dependent opto-electronic properties, which help these materials to be a suitable candidate for designing various opto-electronic devices.<sup>8,9</sup> The intriguing properties of QDs have been explored in a composite system or device through their composites with other materials, which have been explored to various molecules, QDs, 2D nanomaterials, etc. When the QDs are in composite form with biomolecules such materials have been used for bio-imaging. While, the core-shell configuration of QDs have been explored for optoelectronic devices. These QDs have been sensitized with other semiconductors and have created inexpensive, next-generation photovoltaic devices for various applications. In these applications, QDs have been favored because of their size-dependent optical and electronic properties. In this regard, interaction of QDs with surround media or materials is critical for device performance. Although electronic interactions between organic molecules and fluorescent QDs have been well explored, the system where QDs are coupled to other inorganic molecules, such paired system have been elucidated to a lesser extent.

These kinds of interactions are different from those in QDs- molecular systems because the inorganic material possesses a continuum electronic states, while the molecular acceptors have discrete electronic states. When the QDs are coupled with other inorganic materials, the QDs can be used to donate electrons, which have been observed in photovoltaic devices, or these QDs can act as donor/acceptor of the electrons, which have been explored in light emitting diodes (LEDs). In the applications where these QDs are used into devices, the electron transfer is involved with a proper direction of the transfer. As resultant, to understand the factors which use to drive the electron transfer in these composite systems is critical for better understanding and further exploitation of the unique properties of QDs in optoelectronic devices.<sup>10-15</sup>

There are various studies on different kind of QDs, where these QDs have been used as acceptor/donor or both of the electrons. They have also been explored for donor or acceptor in the resonance energy transfer. In recent years researchers have explored various kinds of layered based QDs in place of traditional QDs, e.g., CdS, CdSe, PbS, etc.<sup>16-19</sup> In optoelectronic-based applications these QDs act as light harvesting and charge separation centers, and an important step is the electron transfer or hole transfer from the photoexcited QDs to electron or hole acceptors near the QDs through a nanoscale interface. The overall device efficiency depends on these charge transfer processes with competing loss

<sup>a)</sup> Electronic mail: arunspatel.jnu@gmail.com

<sup>b)</sup> Electronic mail: anirban@jnu.ac.in

pathways. Therefore, understanding and controlling interfacial charge transfer processes is essential for the improvement of QDs based devices. The size of the QDs also plays an important role in the charge transfer process. It has been observed that there is increase in electron transfer rate with decreasing QD size.<sup>20</sup>

In recent years, various 2D layered nanomaterials have been turned in to QDs, and these layered QDs exhibit quite different properties as compared to their 2D structures and as well as bulk counterparts. In this regards, 2D layered structure of transition metal dichalcogenide (TMDC) have also been converted to QDs using various methods. In these TMDC based QDs, MoS<sub>2</sub>, and WS<sub>2</sub> QDs have been studied extensively. They possess interesting optical and electronic properties as their electronic structure can be tuned by tuning their size and surface morphology. These QDs have been used in various applications like sensors, LEDs, photodetectors, cell imaging, etc.<sup>21? -24</sup>

There are a few studies where TMDC QDs have been used as donor of energy in various hybrid systems, due to their photo-luminescence in the UV region. There are numerous studies on the energy transfer/ charge transfer in different set of nanomaterials and there applications in sensors, photodetectors, solar cells, etc. In this work, we have studied the charge transfer in two different kinds of fluorescent materials; fluorescent dye molecules, and QDs. Conventionally, QDs are used as donor/acceptor and the dye molecules as acceptor/donor in the energy transfer, and most of the studies where dye-QDs are used are centered around the energy transfer and its various applications. Here, we have explored the possibility of charge transfer from dye molecules to QDs, which would provide an important insight while developing optoelectronic devices based on fluorescent nanomaterials. In this paper, we have used a common dye molecule; R6G as source of photo-excited electrons, and TMDCs QDs as acceptors for the electrons.

In order to synthesize the QDs and perform this study, various chemicals were used. Molybdenum disulphide (MoS<sub>2</sub>), tungsten disulphide (WS<sub>2</sub>) powder (2 $\mu$ m size), N-Methyl 2-pyrrolidone (NMP), and Rhodamine 6G dye were purchased from Sigma Aldrich. All the chemicals were used as received without further purification.

The TMDC QDs were synthesized using top-down strategy as mentioned in Long et al. with slight modification.<sup>25</sup> In typical synthesis procedure, 0.05 g of TMDC powder was dissolved in 50 mL of NMP solution with constant stirring for 15 hours at 29 °C. The resulting dark suspension was centrifuged at 10,000 rpm for 40 min. The supernatant of the solution was collected and used for further studies.

In our study, prior to exploring charge transfer mechanism, these QDs were characterized by transmission electron microscopy (TEM), fluorescence spectroscopy, and absorption spectroscopy. The TEM images of these QDs were recorded using JEOL-2010 TEM setup operated at 200 kV. The absorption spectra of the QDs were recorded

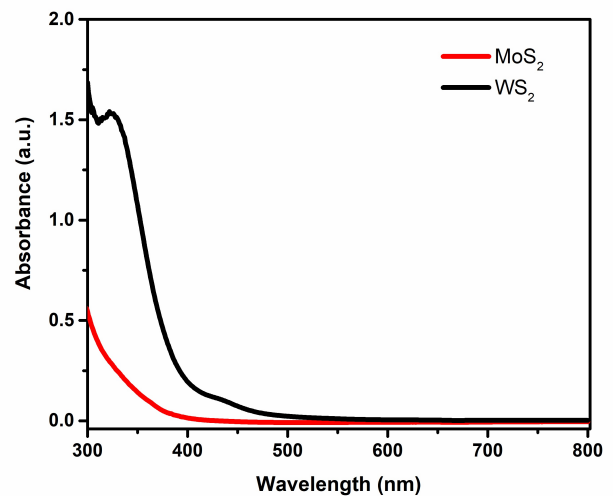


FIG. 1. Absorption spectra of MoS<sub>2</sub>, and WS<sub>2</sub> quantum dots.

using Shimadzu (UV-2450) UV-Vis spectrophotometer. In order to study charge transfer in these TMDCs QDs, the QDs were mixed with a fixed quantity of R6G solution. For charge transfer studies, 0.5 mL aqueous solution of 10<sup>-6</sup> M R6G was further diluted to 3.5 mL, and 1 mL of QDs solution was mixed to R6G solution. In all the samples the NMP and water contents were kept same. The steady state fluorescence spectra of R6G molecules were recorded in absence and presence of TMDCs QDs by using fluorimeter with excitation wavelength of 430 nm. The time resolved fluorescence study was performed using time-correlated single-photon counting module (TC-SPC) (FL920, Edinburgh Instruments, UK) with excitation at 465 nm with diode laser as the excitation source.

The absorption spectra of MoS<sub>2</sub> and WS<sub>2</sub> quantum dots are shown in Fig 1.

A clear absorption peak around 325 nm is observed, which is a characteristic peak of WS<sub>2</sub> quantum dots and it is due to excitonic features of the QDs. Similarly, for MoS<sub>2</sub> QDs a band edge around 380 nm is observed. The color of suspension and the absorption peaks are similar to the previous reported results.<sup>25,26</sup> When the MoS<sub>2</sub> and WS<sub>2</sub> are in the bulk or nanosheet form, they exhibit quite different absorption patterns having two distinct peaks around 600 nm which are known as *A* and *B* excitonic peaks. While in case of QDs these *A* and *B* excitonic peaks disappear and absorption is observed in UV region. The strong blue shift in the absorption of the as-prepared MoS<sub>2</sub> and WS<sub>2</sub> QDs is attributed to the quantum confinement effect and edge effects when the lateral size of the QDs is reduced to few tens of nanometer.<sup>27,28</sup> In order to have insight of the band gaps of these QDs, the Tauc plots of these QDs are drawn. The Tauc plots of the quantum dots are shown in Fig 2.

In case of semiconductors, it has been observed the bandgap increases with decrease in the size of the semiconducting quantum dots.<sup>29</sup> The size dependent bandgap

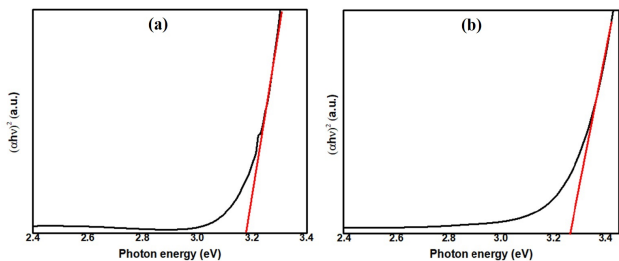


FIG. 2. The Tauc plots of (a) MoS<sub>2</sub>, and (b) WS<sub>2</sub> quantum dots.

is given by following equation:

$$E^* = E_g + \frac{h^2}{8\mu r^2} - \frac{1.8e^2}{4\pi k\epsilon_0 r} \quad (1)$$

where  $E_g$  is the bandgap of the bulk material,  $h$  is the Plank constant,  $\mu$  is the reduced mass of the exciton,  $r$  is radius of the quantum dots,  $e$  is the charge of electron.  $\epsilon_0$  is the permittivity of the free space, and  $k$  is dielectric constant of the material. In this approximation, it is assumed that the particles are spherical in nature, and the motions of electron and hole can be well described in terms of their effective masses. The effect of surface atoms are also ignored in this approximation. For MoS<sub>2</sub>, the reduced mass of exciton is 0.27 times that of the free electron, the bulk bandgap  $E_g$  is 1.29 eV, and the permittivity is about 6.8 times that of free space. The calculated value of the bandgap for MoS<sub>2</sub> quantum dots is found to be 1.9 eV. Similarly for WS<sub>2</sub> the bandgap was found to be 2.7 eV. In case of WS<sub>2</sub>, the reduced mass was taken as 0.146 times that of the free electron mass, the dielectric constant of the material was taken as 4.13 while theoretical calculation of the band gap. In the Equation 1, the second and third terms of the equation are the kinetic energy and electrostatic attraction terms, respectively. It is the kinetic energy term which dominates in general, and results a blue-shift in the bandgap as the size of the quantum dots decreases. As the size of QDs gets smaller the bandgap gets larger because the valence band moves to more positive potential values, and the conduction band moves to more negative potential values. In most of the semi-conducting QDs, the increase in the bandgap is due to the conduction band moving to more negative potential values, and the valence band moves very little (considering potential relative to NHE).<sup>18,29,30</sup> The calculated bandgap is found to be different from the experimentally observed values using Tauc plot which is due to the different size of the QDs, hence there might be variation in the reduced mass of the excitons and the variation in the dielectric constants values at the nanometer scale.

The fluorescence spectra of MoS<sub>2</sub>, and WS<sub>2</sub> are shown in Fig. 3. The QDs show emission in blue region of the electromagnetic spectrum. The origin of this fluorescence emission is quantum confinement effect and the direct bandgap transition in these quantum dots. The emission

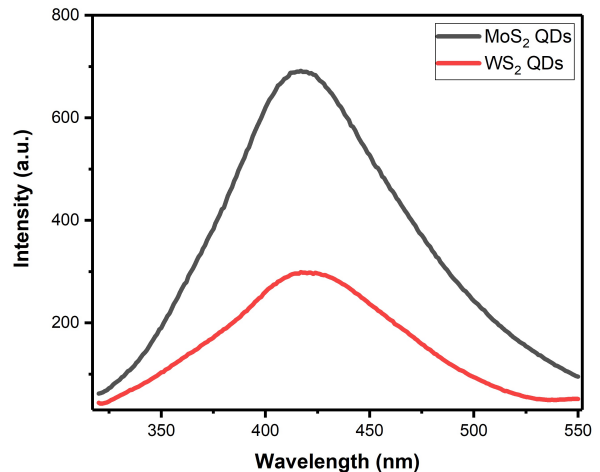


FIG. 3. Fluorescence spectra of MoS<sub>2</sub>, and WS<sub>2</sub> quantum dots.

spectrum has a wide pattern which is due to variation in the size of these QDs. The distribution of these particles size is having broad nature.<sup>31</sup>

The structural properties of MoS<sub>2</sub> and WS<sub>2</sub> quantum dots were explored by using transmission electron microscopy (TEM). Fig. 4 shows the TEM images of the quantum dots. The average size of QDs is of the order of 1.2 nm in case of WS<sub>2</sub> QDs, and 1.7 nm for the MoS<sub>2</sub> QDs.

The photo-response of R6G molecules in the absence as well as in the presence of QDs was examined by using fluorescence spectroscopic techniques. The steady state fluorescence spectra of R6G molecules in the absence and presence of MoS<sub>2</sub> and WS<sub>2</sub> QDs are recorded by fluorimeter using 430 nm excitation wavelength, and emission was recorded in wavelength range of 520-620 nm. The steady state fluorescence spectra of R6G molecules in the absence and presence of MoS<sub>2</sub>, and WS<sub>2</sub> are shown in Fig. 5. The R6G molecules show characteristic emission peak around 550 nm. In Fig. 5, it is found that in the presence of QDs, the fluorescence (FL) intensity of R6G decreases. The decrease in FL intensity confirms quenching due to QDs. The FL quenching are expected to be dynamic or static in nature, which can be confirmed by time resolved fluorescence study. In order to explore the possibility of charge transfer from R6G to QDs, FL lifetime of R6G molecules were recorded in the absence as well as in the presence of the QDs by using time-correlated single photon counting (TCSPC) set-up. The fluorescence lifetime decay spectra of R6G molecules, in the absence and presence of QDs is shown in Fig. 6. Fig. 6 shows the FL lifetime decay curve of R6G molecules in the presence of MoS<sub>2</sub> and WS<sub>2</sub> QDs, and in the absence of the QDs. These decay curves were fitted with exponential decaying

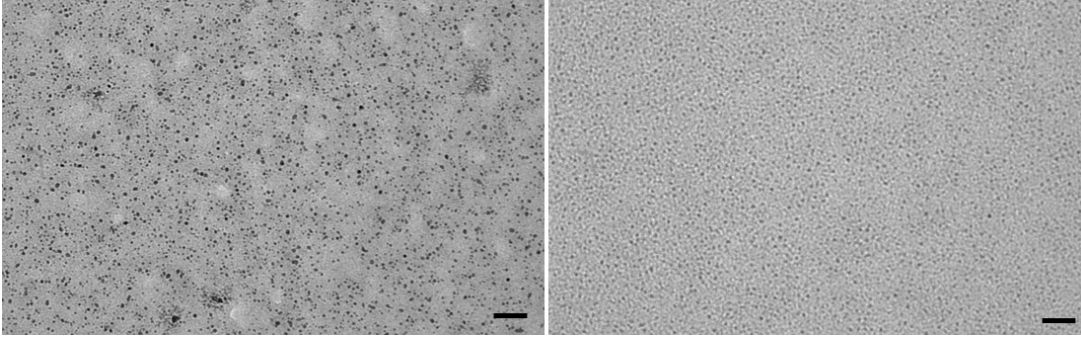


FIG. 4. TEM images of (a) MoS<sub>2</sub>, and (b) WS<sub>2</sub> quantum dots. Scale bar equals to 20 nm.

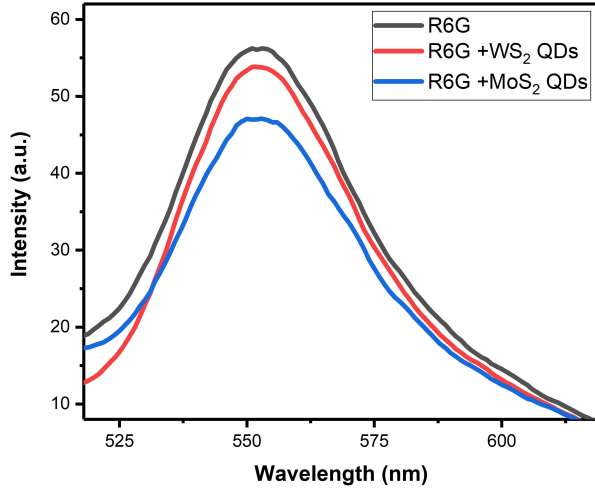


FIG. 5. Fluorescence spectra of R6G molecules in absence and presence of (a) MoS<sub>2</sub>, and (b) WS<sub>2</sub> QDs.

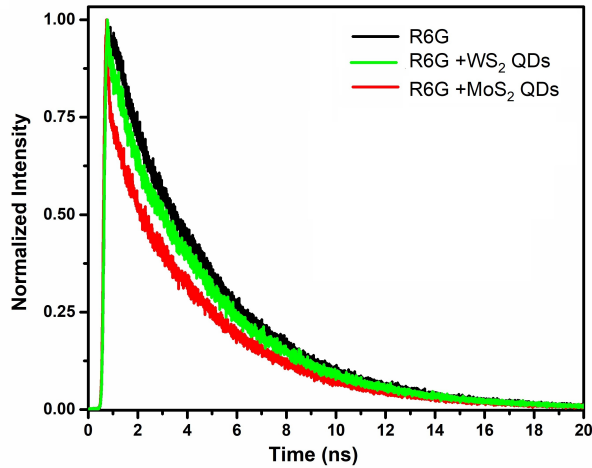


FIG. 6. Fluorescence lifetime decay curves of R6G molecules, in the absence and presence of MoS<sub>2</sub>, and WS<sub>2</sub> quantum dots.

functions of following form:<sup>32</sup>

$$I(t) = \sum_{j=1}^m \alpha_j \exp(-t/\tau_j), \quad (2)$$

where  $m$  is the number of discrete decay components,  $\tau_j$  are the decay times, and  $\alpha_j$  represents the weighing parameter associated with the  $j^{\text{th}}$  decay. It is observed that in presence of QDs, the fluorescence decay curves are steeper in comparison to pure R6G. The decay curve of R6G in absence of QDs is fitted with single-exponential ( $m = 1$ ) decaying function, while in presence of QDs the curves are fitted with bi-exponential ( $m = 2$ ) decaying function. The average fluorescence lifetimes of R6G molecules in absence, as well as in presence of the QDs are calculated. The average fluorescence lifetime of pure R6G was found to be 4.0 ns. In presence of different QDs, the FL lifetime decreases for MoS<sub>2</sub> QDs the FL lifetime is found to be 1.9 ns. The FL lifetime is found to be 3.8 ns in presence of WS<sub>2</sub> QDs. In all cases, in the presence of QDs, there is a significant decrease in the FL lifetime of R6G molecules. In presence of TMDC QDs, the fluorescence intensity as well as the fluorescence lifetime of R6G molecules are found to decrease. The decrease in lifetime indicates that there is some charge/energy transfer from the R6G molecules to QDs. The decrease in the FL lifetime is prominent in case of MoS<sub>2</sub> QDs. In order to understand the possible reasons for decrease in the FL lifetime of the R6G molecules in the presence of QDs, absorption spectra of QDs are plotted along with the emission spectrum of R6G molecules, which is shown in Fig. 7.

In Fig. 7, it is shown that the emission spectrum of R6G does not overlap with the absorption spectra of TMDCs QDs. This cancels the possibilities of energy transfer from R6G to QDs, still there is decrease in the FL intensity as well as FL lifetime of the R6G molecules in presence of QDs, which is due to possibility of charge transfer from the photo-excited R6G molecules to the QDs. In the process of charge transfer, the fluorophores show quenching in the FL intensity, as well as FL lifetimes. Using FL lifetime data, the charge transfer efficiency  $E$  from R6G molecules to TMDC QDs has been

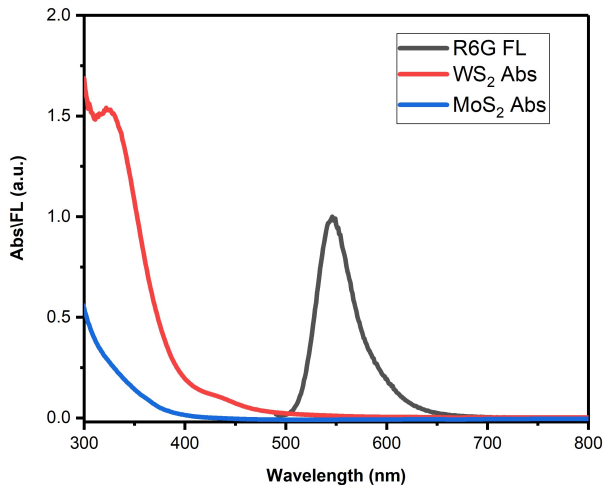


FIG. 7. Absorption spectra of MoS<sub>2</sub>, and WS<sub>2</sub> QDs, along with the fluorescence spectrum of R6G molecules.

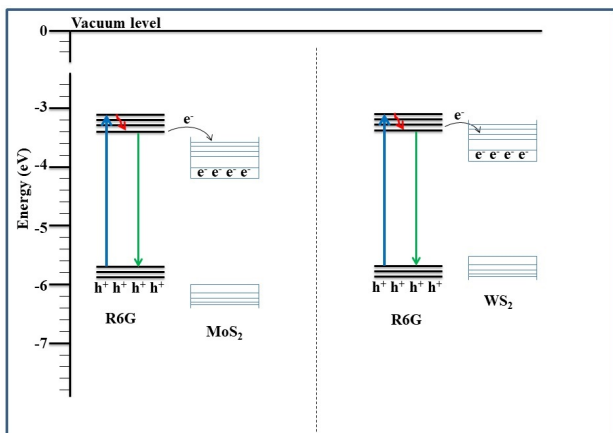


FIG. 8. Schematic of charge transfer from R6G molecules to MoS<sub>2</sub>, WS<sub>2</sub> quantum dots.

calculated using following equation:

$$E = 1 - \frac{\tau_{DA}}{\tau_D}. \quad (3)$$

Here,  $\tau_D$  and  $\tau_{DA}$  are fluorescence lifetimes of R6G molecules, in absence and presence of TMDCs QDs (acceptors), respectively. The charge transfer efficiency, in case of MoS<sub>2</sub> QDs is found to be 53%. For WS<sub>2</sub>, the efficiency is found to be 3%.

The mechanism of charge transfer from R6G molecules to TMDCs QDs is illustrated in Fig. 8, and Fig. 9. The schematic of energy levels of R6G, MoS<sub>2</sub> and WS<sub>2</sub> quantum dots are shown in Fig. 8, and a schematic of charge transfer in the QDs are shown in Fig. 9.

It has been previously observed that the dye can be brought to excited state by absorbing the photons of suitable wavelength and further the excited dye can transfer electrons to the conduction band of adjacent semiconducting materials, in this way the dye can be degraded

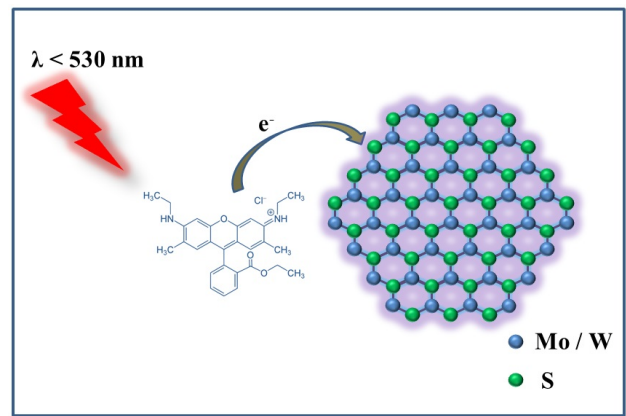


FIG. 9. Schematic of charge transfer from R6G molecules to MoS<sub>2</sub>, WS<sub>2</sub> quantum dots.

by the reactive oxygen species.<sup>33</sup> Here, in this study, we used R6G dye molecules which has redox potentials 1.2 V and -1.1 V vs NHE for ground state (HOMO) and excited state (LUMO), respectively.<sup>33</sup> The energy levels of R6G in its ground state and excited state versus vacuum is calculated using equation  $E(\text{eV}) = -4.5 - E_{NHE}$  and the respective energy levels are -5.7 eV and -3.4 eV, for ground and excited state, respectively. The optical band gap of R6G dye molecules is of the order of 2.3 eV, which corresponds to 540 nm of the wavelength. The potential of the valence band and conduction band of MoS<sub>2</sub> are found to be -6.0 eV and -4.2 eV, respectively. Similarly, the valence band and conduction band energy levels of WS<sub>2</sub> are found to be at -5.48 eV, and -3.93 eV, respectively.<sup>34</sup> From these energy levels, it is observed that by absorbing photons of wavelength  $\lambda < 530$  nm, R6G molecules make transition into an excited state R6G\* and the energy differences between R6G\* state to the conduction bands of QDs provide a thermodynamically favourable condition for the transfer of electrons from LUMO of R6G to the conduction band of MoS<sub>2</sub> and WS<sub>2</sub> QDs. The energy difference between LUMO of R6G and conduction band of MoS<sub>2</sub> is 0.8 eV and for WS<sub>2</sub>, the difference is 0.53 eV. The energy difference is maximum in case of MoS<sub>2</sub> which favours the charge transfer from R6G molecules in the excited state to the conduction band of the MoS<sub>2</sub> as compared to the WS<sub>2</sub>. Therefore the charge transfer efficiency is maximum (53%) in MoS<sub>2</sub> QDs. This study can be further extended to other quantum dots and 2D materials and the efficiency of charge transfer can be tailored by selecting appropriate materials.

In summary, the MoS<sub>2</sub> and WS<sub>2</sub> QDs were synthesized using ultrasonication method. The photo-induced charge transfer between fluorescent R6G molecules and TMDC QDs of MoS<sub>2</sub> and WS<sub>2</sub> was studied using fluorescence spectroscopic techniques. The QDs of MoS<sub>2</sub> and WS<sub>2</sub> were used as acceptors for charge transfer, which could be further explored to developing QDs-molecules based optoelectronic devices. Maximum charge transfer efficiency was observed in case of MoS<sub>2</sub> QDs which was due to a

wide energy difference between the LUMO of the R6G molecules and the conduction energy level of the MoS<sub>2</sub> QDs, it had provided a thermodynamically favourable condition of the charge transfer.

Authors acknowledge the AIRF, JNU for TRFS, and TEM characterizations. Authors are also thankful to Dr. Jaydeep Bhattacharya of the School of Biotechnology, JNU for absorption and fluorescence studies.

- <sup>1</sup>Q. Xu, J. Gao, S. Wang, Y. Wang, D. Liu, and J. Wang, "Quantum dots in cell imaging and their safety issues," *Journal of Materials Chemistry B* **9**, 5765–5779 (2021).
- <sup>2</sup>M. Li, J. Yan, X. Zhao, T. Ma, A. Zhang, S. Chen, G. Shen, G. M. G. Khalaf, J. Zhang, C. Chen, *et al.*, "Synergistic enhancement of efficient perovskite/quantum dot tandem solar cells based on transparent electrode and band alignment engineering," *Advanced Energy Materials*, 2400219 (2024).
- <sup>3</sup>L. Wang, W. Li, L. Yin, Y. Liu, H. Guo, J. Lai, Y. Han, G. Li, M. Li, J. Zhang, *et al.*, "Full-color fluorescent carbon quantum dots," *Science advances* **6**, eabb6772 (2020).
- <sup>4</sup>S. Sadeghi, S. Khabbaz Abkenar, C. W. Ow-Yang, and S. Nizamoglu, "Efficient white leds using liquid-state magic-sized cdse quantum dots," *Scientific reports* **9**, 1–9 (2019).
- <sup>5</sup>X. Li, Y. Wu, S. Zhang, B. Cai, Y. Gu, J. Song, and H. Zeng, "Cspx3 quantum dots for lighting and displays: room-temperature synthesis, photoluminescence superiorities, underlying origins and white light-emitting diodes," *Advanced Functional Materials* **26**, 2435–2445 (2016).
- <sup>6</sup>Y. Xue, F. Yang, J. Yuan, Y. Zhang, M. Gu, Y. Xu, X. Ling, Y. Wang, F. Li, T. Zhai, *et al.*, "Toward scalable pbs quantum dot solar cells using a tailored polymeric hole conductor," *ACS Energy Letters* **4**, 2850–2858 (2019).
- <sup>7</sup>L. Meng, Q. Xu, J. Zhang, and X. Wang, "Colloidal quantum dot materials for next-generation near-infrared optoelectronics," *Chemical Communications* (2024).
- <sup>8</sup>X. Li, M. Rui, J. Song, Z. Shen, and H. Zeng, "Carbon and graphene quantum dots for optoelectronic and energy devices: a review," *Advanced Functional Materials* **25**, 4929–4947 (2015).
- <sup>9</sup>A. Litvin, I. Martynenko, F. Purcell-Milton, A. Baranov, A. Fedorov, and Y. Gun'ko, "Colloidal quantum dots for optoelectronics," *Journal of Materials Chemistry A* **5**, 13252–13275 (2017).
- <sup>10</sup>W. R. Algar and U. J. Krull, "Quantum dots as donors in fluorescence resonance energy transfer for the bioanalysis of nucleic acids, proteins, and other biological molecules," *Analytical and bioanalytical chemistry* **391**, 1609–1618 (2008).
- <sup>11</sup>Q. Wang, W.-Q. Chen, X.-Y. Liu, Y. Liu, and F.-L. Jiang, "Thermodynamic implications and time evolution of the interactions of near-infrared pbs quantum dots with human serum albumin," *ACS omega* **6**, 5569–5581 (2021).
- <sup>12</sup>H. Zhu, H. Zhang, and Y. Xia, "Planar is better: monodisperse three-layered mos2 quantum dots as fluorescent reporters for 2, 4, 6-trinitrotoluene sensing in environmental water and luggage cases," *Analytical chemistry* **90**, 3942–3949 (2018).
- <sup>13</sup>C. N. Lima, W. F. Oliveira, P. M. Silva, P. E. Cabral Filho, K. Juul-Madsen, P. Moura, T. Vorup-Jensen, and A. Fontes, "Mannose-binding lectin conjugated to quantum dots as fluorescent nanotools for carbohydrate tracing," *Methods and Applications in Fluorescence* **10**, 025002 (2022).
- <sup>14</sup>Z. Wu, P. Liu, W. Zhang, K. Wang, and X. W. Sun, "Development of inp quantum dot-based light-emitting diodes," *ACS Energy Letters* **5**, 1095–1106 (2020).
- <sup>15</sup>A. Rani, K. Singh, A. S. Patel, A. Chakraborti, S. Kumar, K. Ghosh, and P. Sharma, "Visible light driven photocatalysis of organic dyes using sno2 decorated mos2 nanocomposites," *Chemical Physics Letters* **738**, 136874 (2020).
- <sup>16</sup>P. R. Kharangarh, N. M. Ravindra, G. Singh, and S. Umapathy, "Synthesis of luminescent graphene quantum dots from biomass waste materials for energy-related applications—an overview," *Energy Storage* **5**, e390 (2023).
- <sup>17</sup>Sariga, A. M. Babu, S. Kumar, R. Rajeev, D. A. Thadathil, and A. Varghese, "New horizons in the synthesis, properties, and applications of mxene quantum dots," *Advanced Materials Interfaces* **10**, 2202139 (2023).
- <sup>18</sup>Z. Gan, L. Liu, H. Wu, Y. Hao, Y. Shan, X. Wu, and P. K. Chu, "Quantum confinement effects across two-dimensional planes in mos2 quantum dots," *Applied Physics Letters* **106**, 233113 (2015).
- <sup>19</sup>M. Guo, Z. Xing, T. Zhao, Z. Li, S. Yang, and W. Zhou, "Ws2 quantum dots/mos2@wo3-x core-shell hierarchical dual z-scheme tandem heterojunctions with wide-spectrum response and enhanced photocatalytic performance," *Applied Catalysis B: Environmental* **257**, 117913 (2019).
- <sup>20</sup>H. Zhu, Y. Yang, K. Wu, and T. Lian, "Charge transfer dynamics from photoexcited semiconductor quantum dots," *Annual review of physical chemistry* **67**, 259–281 (2016).
- <sup>21</sup>Y. Yan, C. Zhang, W. Gu, C. Ding, X. Li, and Y. Xian, "Facile synthesis of water-soluble ws2 quantum dots for turn-on fluorescent measurement of lipoic acid," *The Journal of Physical Chemistry C* **120**, 12170–12177 (2016).
- <sup>22</sup>A. Ghorai, S. Bayan, N. Gogurla, A. Midya, and S. K. Ray, "Highly luminescent ws2 quantum dots/zno heterojunctions for light emitting devices," *ACS applied materials & interfaces* **9**, 558–565 (2017).
- <sup>23</sup>V. K. Singh, S. M. Yadav, H. Mishra, R. Kumar, R. Tiwari, A. Pandey, and A. Srivastava, "Ws2 quantum dot graphene nanocomposite film for uv photodetection," *ACS Applied Nano Materials* **2**, 3934–3942 (2019).
- <sup>24</sup>Y. Guo and J. Li, "Mos2 quantum dots: synthesis, properties and biological applications," *Materials Science and Engineering: C* **109**, 110511 (2020).
- <sup>25</sup>H. Long, L. Tao, C. P. Chiu, C. Y. Tang, K. H. Fung, Y. Chai, and Y. H. Tsang, "The ws2 quantum dot: preparation, characterization and its optical limiting effect in polymethylmethacrylate," *Nanotechnology* **27**, 414005 (2016).
- <sup>26</sup>J. N. Coleman, M. Lotya, A. O'Neill, S. D. Bergin, P. J. King, U. Khan, K. Young, A. Gaucher, S. De, R. J. Smith, *et al.*, "Two-dimensional nanosheets produced by liquid exfoliation of layered materials," *Science* **331**, 568–571 (2011).
- <sup>27</sup>B. Li, L. Jiang, X. Li, P. Ran, P. Zuo, A. Wang, L. Qu, Y. Zhao, Z. Cheng, and Y. Lu, "Preparation of monolayer mos2 quantum dots using temporally shaped femtosecond laser ablation of bulk mos2 targets in water," *Scientific Reports* **7**, 1–12 (2017).
- <sup>28</sup>N. Liu, P. Kim, J. H. Kim, J. H. Ye, S. Kim, and C. J. Lee, "Large-area atomically thin mos2 nanosheets prepared using electrochemical exfoliation," *ACS nano* **8**, 6902–6910 (2014).
- <sup>29</sup>X. Wu, J. Fan, T. Qiu, X. Yang, G. Siu, and P. K. Chu, "Experimental evidence for the quantum confinement effect in 3 c-sic nanocrystallites," *Physical review letters* **94**, 026102 (2005).
- <sup>30</sup>F. Parsapour, D. Kelley, S. Craft, and J. Wilcoxon, "Electron transfer dynamics in mos2 nanoclusters: Normal and inverted behavior," *The Journal of chemical physics* **104**, 4978–4987 (1996).
- <sup>31</sup>H. D. Ha, D. J. Han, J. S. Choi, M. Park, and T. S. Seo, "Dual role of blue luminescent mos2 quantum dots in fluorescence resonance energy transfer phenomenon," *Small* **10**, 3858–3862 (2014).
- <sup>32</sup>A. S. Patel, H. Sahoo, and T. Mohanty, *Applied Physics Letters* **105**, 063112 (2014).
- <sup>33</sup>Y. Li, W. Xie, X. Hu, G. Shen, X. Zhou, Y. Xiang, X. Zhao, and P. Fang, "Comparison of dye photodegradation and its coupling with light-to-electricity conversion over tio2 and zno," *Langmuir* **26**, 591–597 (2010).
- <sup>34</sup>S. Mukherjee, R. Maiti, A. K. Katiyar, S. Das, and S. K. Ray, "Novel colloidal mos2 quantum dot heterojunctions on silicon platforms for multifunctional optoelectronic devices," *Scientific reports* **6**, 1–11 (2016).